Article

*Discovery Medicine* 2023; 35(177): 576–589
https://doi.org/10.24976/Discov.Med.202335177.58

# $H_2S$ Alleviates Propofol-Induced Impaired Learning and Memory by Promoting Nuclear Translocation of *Nrf2* and Inhibiting Apoptosis and Pyroptosis in Hippocampal Neurons

Zhenyu Li[1], Yanfang Wang[2], Man Feng[3], Xue Wang[3], Baofeng Gao[1,*]

[1]Department of Anesthesiology, Shandong Provincial Third Hospital, 250001 Jinan, Shandong, China
[2]Department of Anesthesiology, Jinan Fourth People's Hospital, 250031 Jinan, Shandong, China
[3]Department of Pathology, The Third Affiliated Hospital of Shandong First Medical University, Affiliated Hospital of Shandong Academy of Medical Sciences, 250031 Jinan, Shandong, China
*Correspondence: gbf1200@163.com (Baofeng Gao)
Published: 1 August 2023

**Background: Repeated exposure to propofol can affect their learning and memory functions, but the mechanism remains unclear. The current study aimed to investigate the mechanism underlying the effect of hydrogen sulfide ($H_2S$) on the alleviation of propofol-induced learning and memory impairment, mediated by promoting nuclear translocation of the nuclear factor erythroid 2-related factor 2 (*Nrf2*) and inhibiting apoptosis and pyroptosis in hippocampal neurons.**

**Methods: Rats used in this study were successively exposed to 200 mg/kg propofol for 8 consecutive weeks, followed by inhalation of 10, 40 or 80 ppm $H_2S$. Subsequently, the effects of different concentrations of $H_2S$ on learning and memory were assessed using the water maze assay. Additionally, the effects of $H_2S$ on cell apoptosis and pyroptosis and nuclear translocation of *Nrf2* in hippocampal neurons were also determined. Furthermore, NaHS (200 µmol/L) was used as an *in vitro* donor for $H_2S$, and rescue experiments were carried out following *Nrf2* knockdown in H19-7 cells. Moreover, *Nrf2* function was inhibited following treatment with an intraperitoneal injection of ML385 (30 mg/kg) in the rats. The effects of $H_2S$ on reactive oxygen species (ROS) generation, cell apoptosis, and pyroptosis in propofol-treated and *Nrf2*-deficient H19-7 cells were also investigated.**

**Results: Exposure to propofol for 8 weeks affected the ability of the rats to find underwater platforms ($p < 0.01$). Further, the exposure induced cell apoptosis and NLR family pyrin domain containing 3 (NLRP3)-related pyroptosis ($p < 0.01$). Although inhalation of 10 ppm $H_2S$ did not attenuate the aforementioned effects ($p > 0.05$), exposure to 40 and 80 ppm $H_2S$ significantly alleviated propofol-induced injury in the hippocampal neurons ($p < 0.01$). However, the protective effect of 80 ppm $H_2S$ was more obvious as compared to that of the other two doses ($p < 0.01$). In addition, *Nrf2* knockdown aggravated the propofol-induced cell pyroptosis and apoptosis as well as reversed the protective effect of $H_2S$ against these processes ($p < 0.01$). *In vivo* experiments in this study demonstrated that *Nrf2* inhibition abrogated the protective effects of $H_2S$ inhalation against learning and memory impairment as well as propofol-induced cell apoptosis and pyroptosis in rats ($p < 0.01$).**

**Conclusions: $H_2S$ could attenuate propofol-induced damage in hippocampal neurons by promoting the nuclear translocation of *Nrf2* and inhibiting cell apoptosis and pyroptosis.**

**Keywords:** propofol; hippocampal neurons; hydrogen sulfide; *Nrf2*; apoptosis; pyroptosis

## Introduction

Propofol is a short-acting anesthetic that is commonly used for epidural anesthesia and as an inhalation anesthetic [1,2]. It is often used in gastroscopy and colonoscopy, particularly in patients who require repeated gastroenteroscopy [3,4]. It has been reported that repeated exposure to propofol can damage the hippocampal neurons in children, thus affecting their learning and memory functions [5,6]. Additionally, a previous study reported that propofol exhibited several adverse effects on neurological function in the elderly population [7]. However, the mechanism of propofol-induced hippocampal injury remains unclear.

It has been reported that propofol induces oxidative stress, which eventually leads to neuronal cell apoptosis *in vitro*, while the inhibition of reactive oxygen species (ROS) alleviates the neurotoxicity of propofol [8–10]. ROS is considered a key factor in the activation of the NLR family pyrin domain containing 3 (NLRP3) [11], which not only induces an inflammatory response but also cleaves and releases the activated caspase-1 to induce pyroptosis [12]. In turn, caspase-1 cleaves gasdermin (GSDM) whereas N-GSDM disrupts the integrity and permeability of the cell membrane, which results in cell rupture [13]. A previous study suggested that a high dose of propofol could induce

NLRP3-dependent macrophage pyroptosis [14]. However, it remains elusive whether repeated exposure to propofol induces pyroptosis in the hippocampal neurons. Further, its underlying mechanism of action also remains unclear.

Under physiological conditions, hydrogen sulfide ($H_2S$) commonly exists in the form of $HS^-$ ion. A study demonstrated that $H_2S$ could inhibit NLRP3-dependent pyroptosis in bronchial epithelial cells [15]. In corroboration, another study also revealed that $H_2S$ could attenuate pyroptosis and protect kidney against ischemic kidney injury [16]. Nuclear factor erythroid 2-related factor 2 (*Nrf2*) is a key antioxidant gene *in vivo*. The nuclear translocation of the *Nrf2* protein induces an antioxidant response [17,18], thereby inhibiting the activation of NLRP3 and pyroptosis [19]. *Nrf2* is also an important signaling molecule in microbial infections [20–23]. For example, the study of Harvey *et al*. [20] suggested that *Nrf2* up-regulated the macrophage receptor with collagenous structure (MARCO). Furthermore, they reported that *Nrf2* changed the composition of the gut microbiota and colorectal cancer development [21]. Moreover, $H_2S$ can also activate *Nrf2*. Notably, $H_2S$ reduced the risk of cardiovascular disease in patients with diabetes by activating the *Nrf2* pathway [24]. Furthermore, another study demonstrated that $H_2S$ could also inhibit doxorubicin-induced and ROS-associated myocardial fibrosis by activating *Nrf2* [25]. However, whether $H_2S$ alleviates propofol-induced pyroptosis in hippocampal neurons by activating the *Nrf2* pathway has not been investigated previously.

The current study mainly focused on cell apoptosis and pyroptosis to test the effect of $H_2S$ on propofol-induced hippocampal neuron damage and to elucidate the possible protective mechanism of $H_2S$ on learning and memory in rats through *Nrf2*. Our results could offer insights regarding the basic theory for the clinical application of propofol as well as novel strategies for preventing and mitigating propofol-related neurotoxicity.

## Materials and Methods

### *Animal Treatment*

Fifty Sprague Dawley (SD) rats (10 weeks; 300–350 g, Shandong Experimental Animal Center, Jinan, China) were randomly assigned into five groups: Control; propofol (Pro), Pro+$H_2S$-10, Pro+$H_2S$-40, Pro+$H_2S$-80. Rats in Pro, Pro+$H_2S$-10, Pro+$H_2S$-40 and Pro+$H_2S$-80 groups were injected intraperitoneally with 200 mg/kg of propofol (Catalogue no. H20084531, Jiuxu Pharmaceutical Co., Ltd., Jiuxu, China) once every 7 days for 8 weeks [7]. At 2 h after each propofol injection, the rats were treated with $H_2S$ inhalation. Subsequently, the rats were placed in an 8 L glass chamber. The inhaled air was composed of a mixture of air and $H_2S$ (batch no. 202211213, Wuhan New Radar Special Gas Co., Ltd., Wuhan, China). The $H_2S$ intake volume was adjusted by detecting the concentration of $H_2S$ at the air outlet. Therefore, the concentration of $H_2S$ in the device was set at 10, 40, or 80 ppm [26]. Rats inhaled $H_2S$ for 8 h/day for 3 consecutive days until the next propofol injection and $H_2S$ re-inhalation were administered. Rats were anesthetized with 75 mg/kg ketamine (i.p.) and 5.0 mg/kg diazepam (i.p.). The method of euthanasia was i.p. injection of pentobarbital Na (150 mg/kg).

In the subsequent experiments, forty rats were divided into Control, Pro, Pro+$H_2S$ and Pro+$H_2S$+ML385 groups. Rats in the negative control (NC), Pro and Pro+$H_2S$ groups received respective treatment as described above. Rats in Pro+$H_2S$+ML385 group were treated with 200 mg/kg of propofol, 40 ppm $H_2S$ and 30 mg/kg ML385 for 24 h. For the inhibition of *Nrf2* protein expression *in vivo*, *Nrf2* function was blocked following intraperitoneal injection of ML385 (30 mg/kg dissolved in dimethyl sulfoxide (DMSO); Catalogue no. M8692, Abmole Bioscience Inc., Houston, TX, USA) 30 minutes before each $H_2S$ inhalation [27]. Humane endpoints included rapid weight loss, weakness, loss of appetite, and untreatable infections. The maximum percent body weight loss of animals was 6% at the end of the experiment. The experimental protocols complied with the revised Animals (Scientific Procedures) Act 1986 in the UK, and they were approved by the Animal Care Committee of Shandong Provincial Third Hospital (No. DWKYLL-2020008).

### *Morris Water Maze Assay*

The temperature of the water maze (Catalogue no. XR-XM101, Xinsoft Information Technology Co., Ltd., Shanghai, China) was adjusted to 25 $\pm$ 1 °C. The diameter and height of the swimming maze were 160 and 40 cm, respectively. In one quadrant of the pool, a platform was hidden at 0.5 cm underwater. The rats were placed sequentially against a wall in the water maze. Time recording was ended for a rat when it landed on the platform area within 90 sec. When the rat could not board the platform area within 90 sec, it was gently guided onto the platform with a stick and could stay for 30 sec for all rats. All the rats were trained four times. The interval between each trial was >5 min. Subsequently, the underwater platform was withdrawn, and the animals were relocated to the same quadrant to record the movement trajectory.

### *Nissl Staining*

The rats were euthanized by decapitation using a guillotine after administration of ketamine/xylazine solution for anesthesia (75/10 mg/kg; i.p., Sigma-Aldrich, Merck KGaA, Saint Louis, MO, USA). Complete cardiac arrest and pupil dilation were considered to be indicative of death. Following euthanasia, the hippocampus was removed from each rat. Freshly obtained hippocampal tissues were fixed in 10% neutral formalin and embedded in paraffin. Subsequently, the tissue samples were cut into 6 µm thick sections, deparaffinized, and rinsed with distilled water. The

tissue sections were then put into a staining jar with Toluidine Blue (Catalogue. no. ZY92, Zeye Bio, Shanghai, China), which was followed by incubation at 50–60 °C for approximately 30 min. The samples were first rinsed lightly with distilled water and thereafter with 70% ethanol. Subsequently, the tissue sections were desiccated with 95% ethanol, dehydrated with absolute ethanol, transparentized in xylene, and sealed with neutral gum. The tissue sections were obtained under a microscope (Keyence) and the images were obtained.

### *TUNEL Assay*

The hippocampal tissues were fixed using 10% neutral formalin. Thereafter, they were sectioned and deparaffinized. Following washing (5 min/wash) with xylene, the tissues were rehydrated with a descending ethanol gradient. The tissues were treated with proteinase K for 15 min at 37 °C. Subsequently, the samples were incubated with 100 µL TdT-mediated dUTP-biotin nick end labeling (TUNEL) reagent (Roche Diagnostics) and then incubated with 100 µL streptavidin-labeled HRP antibody (dilution; 1:500; Catalogue no. N100, Thermo Fisher, Cleveland, OH, USA) for 30 min. This was followed by staining with 100 µL DAB for 10 min. When a light brown background was observed under the microscope, the samples were counterstained with hematoxylin for 3 sec. Following dehydration, the tissues were treated with xylene and sealed with neutral gum.

### *Cell Culture*

The rat hippocampal neuron cell line H19-7 (cat. no. CRL-2526, ATCC, Manassas, VA, USA) was maintained in DMEM (Batch No. 11965092, Gibco, Carlsbad, CA, USA) that was supplemented with 10% FBS, 100 mg/mL streptomycin, and 100 U/mL penicillin (Batch No. 516106-20MLCN, Millipore Sigma, Burlington, MA, USA). H19-7 cells were subjected to short tandem repeat (STR) validation and mycoplasma testing ang confirmed to be uncontaminated. To select the optimal experimental concentration, H19-7 cells were exposed to 50, 100, 150 and 200 µmol/L propofol for 24 h [28]. Following incubation in the presence of propofol, H19-7 cells were co-treated with 100, 200 or 400 µmol/L NaHS ($H_2S$ donor) for 24 h. Next, cells were divided into negative control (NC), Pro, Pro+si*Nrf2*, Pro+$H_2S$, Pro+si*Nrf2*+$H_2S$ groups. Cells in NC group received no treatment; Cells in Pro group were treated with 150 µmol/L propofol for 24 h; Cells in Pro+si*Nrf2* group were treated with 150 µmol/L propofol and si*Nrf2* transfection for 24 h; Cells in Pro+$H_2S$ group were treated with 150 µmol/L propofol and 200 µmol/L NaHS for 24 h; Cells in Pro+si*Nrf2*+$H_2S$ group were treated with 150 µmol/L propofol, si*Nrf2* transfection and 200 µmol/L NaHS for 24 h.

### *Cell Transfection*

The small interfering (si) RNA clone targeting *Nrf2*, and the corresponding negative control (NC) clone were synthesized by Shanghai GenePharma Co., Ltd. (Shanghai, China).

The sequences used were as follows: For si*Nrf2*, sense, 5′-GCCUGUAAGUCCUGGUCAUTT-3′ and antisense, 5′-AUGACCAGGACUUACAGGCTT-3′; and for NC, sense, 5′-UUCUCCGAACGUGUCACGUTT-3′ and antisense, 5′-ACGUGACACGUUCGGAGAATT-3′. A total of 50 pmol (0.67 µg) of each clone was diluted in 25 µL serum-free DMEM (reagent A). Subsequently, 1 µL Entranster TM-R4000 (Engreen Biosystem Co., Ltd., Beijing, China) was mixed with 24 µL serum-free DMEM (reagent B), and 25 µL of both the reagents (reagent A and reagent B) were mixed thoroughly by aspirating 10 times with a pipette. The mixture was allowed to stand for 15 min. Finally, 50 µL of the above transfection mixture was added to the cells that were cultured in 0.45 mL of complete medium. The cells were collected after 36 h.

### *Determination of ROS Levels in Cells and Brain Tissue*

In order to evaluate the ROS levels in cells, a solution of DCFH-DA was prepared by diluting the stock solution with DMSO. Following a wash with phosphate buffer saline (PBS), the cells were incubated in DMSO containing 10 µM DCFH-DA at 37 °C for 30 min and then collected and analyzed by flow cytometry to determine the mean fluorescence of 10,000 cells. To assess the ROS levels in brain tissue, the tissue was homogenized in 40 mM Tris-HCl buffer and then incubated with 10 µM 2′, 7′ dichlorofluorescein diacetate in Tris-HCl buffer. After incubation in the dark at 37 °C for 15 min, the fluorescence intensity (FI) was measured at an excitation wavelength of 485 nm and an emission wavelength of 525 nm using a microplate reader.

### *CCK-8 Assay*

For the cell counting kit-8 (CCK-8) assay, 100 µL of cell suspension, which had a density of $5 \times 10^4$ cells/mL, was added to 96-well plates. Each well was replicated five times. The plates were incubated for 24–48 h before 10 µL of CCK-8 solution was added to each well. The plates were then gently shaken for 1 min at 37 °C to ensure uniform mixing. Furthermore, the cells were incubated for 2 h to facilitate dehydrogenation. Finally, the optical density was measured with a microplate reader (Synergy H1 Hybrid Multi-Mode, BioTek Instruments, Inc., Winooski, VT, USA) at 450 nm.

### *Flow Cytometry*

Cells were collected and trypsinized without ethylene diamine tetraacetic acid (EDTA). The PBS-washed cells underwent two rounds of centrifugation for 5 min at 1000 ×g at 4 °C, resulting in a total of $5 \times 10^5$ cells. These cells

were mixed with 500 µL of binding buffer, and 5 µL each of Annexin V-FITC and PI (Batch No. C1062L, Beyotime Institute of Biotechnology, Shanghai, China) were added to them. The mixture was incubated in the dark at 4 °C for 15 min to allow for the detection of apoptotic cells. Flow cytometry (BD FACSCalibur™; BD Biosciences, Beijing, China) was performed within 30 min to determine cell apoptosis. Normal cells were used to set the cross-gate position and for fluorescence compensation.

### *Western Blot Analysis*

Cells were collected and incubated on ice with Radio Immunoprecipitation Assay (RIPA) lysis solution for 30 min. Total proteins were isolated after centrifugation at 12,000 ×g for 20 min at 4 °C. Cytoplasmic and nuclear protein extracts were separated using the Minute™ Cytoplasmic and Nuclear Fractionation kit (Catalogue. no. SC-003, Invent Biotechnologies, Inc., Plymouth, MN, USA). Bicinchoninic acid (BCA) kit (cat. no. P0012S, Beyotime, Shanghai, China) was used for the quantitative detection of the proteins. Further, 10% SDS-PAGE was used to separate the proteins. Thereafter, the membranes were incubated with primary rabbit antibodies at a dilution of 1:1000 and kept overnight at a temperature of 4 °C. The following primary antibodies were used: anti-NLRP3 (1:1000, catalogue no. ab263899, Abcam, Cambridge, MA, USA), anti-pro-caspase-1 (1:2000, catalogue no. ab108333, Abcam, Cambridge, MA, USA), anti-cleaved caspase-1 (1:2000, catalogue no. ab256469, Abcam, Cambridge, MA, USA), anti-GSDM-D (1:2000, catalogue no. ab219800, Abcam, Cambridge, MA, USA), anti-*Nrf2* (1:2000, catalogue no. ab92946, Abcam, Cambridge, MA, USA), Glyceraldehyde-3- phosphate dehydrogenase (GAPDH) (1:1000, catalogue no. ab181602, Abcam, Cambridge, MA, USA) and anti-H3 (1 µg/mL, catalogue no. ab8580, Abcam, Cambridge, MA, USA; all from Abcam, Cambridge, MA, USA). The membranes were washed twice with TBS containing 0.1% Tween and incubated with the appropriate secondary antibody (at a dilution of 1:2000; Catalogue no. ab6721, Abcam, Cambridge, MA, USA) for 2 h at 37 °C. Thereafter, the membranes were washed three times with TBS containing 0.1% Tween 20 (TBST). Finally, the protein bands were visualized using an ECL kit (Beijing Solarbio Science & Technology Co., Ltd, Beijing, China) and analyzed using Image Pro Plus Version 6.0 (Media Cybernetics, Inc. Rockville, MD, USA).

### *2',7'-Dichlorofluorescein (DCF) Assay*

Fresh frozen sections (20 µm) or cells were directly immersed in $H_2$DCF-DA (10 µmol/L; Invitrogen, Thermo Fisher Scientific, Inc., Cleveland, OH, USA). Thereafter, they were fixed and incubated in the dark for 1 h. The fluorescence intensity was measured at 485 nm (excitation) and 538 nm (emission) with a a microplate reader (Synergy H1 Hybrid Multi-Mode, BioTek Instruments, Inc., Winooski, VT, USA).

### *Statistical Analysis*

The mean ± standard deviation (SD) was used to represent the data. To compare the differences among multiple groups, analysis of variance (ANOVA) was employed followed by Tukey's multiple comparison test. Further, an unpaired *t*-test was used to compare the differences between the two groups. GraphPad Prism version 7.0 (GraphPad Software Inc., San Diego, CA, USA) was used for all the statistical analyses. A statistically significant difference was determined by a $p$-value $< 0.01$.

## Results

### *$H_2S$ Alleviates Propofol-Induced Learning and Memory Dysfunction*

To elucidate the effects of $H_2S$ on propofol-induced neurotoxicity *in vivo*, rats were divided into the following five groups (n = 5): control, propofol (Pro), Pro+$H_2S$-10, Pro+$H_2S$-40, and Pro+$H_2S$-80 groups. Rats were treated with 10, 40 and 80 ppm $H_2S$ following propofol exposure. The water maze test results showed that the escape latency of rats in the Pro group increased significantly as compared to normal rats ($p < 0.01$). Although 10 ppm $H_2S$ had no significant effect on the rats in the Pro group ($p > 0.05$), treatment with 40 and 80 ppm $H_2S$ notably reduced their escape latency ($p < 0.01$). Additionally, the escape latency of rats in the Pro+$H_2S$-80 group was significantly lower as compared to that in rats of the Pro+$H_2S$-40 group (Fig. 1A,B, $p < 0.01$). Furthermore, the percentage of time that the rats spent in the target quadrant and the number of crossing platforms were markedly decreased in the Pro group as compared to the control group ($p < 0.01$). The inhalation of 40 and 80 ppm $H_2S$ had a protective effect on the learning and memory ability of rats, and the effect of 80 ppm $H_2S$ was significantly better than that of 40 ppm (Fig. 1C,D, $p < 0.01$). While hippocampal neurons are the main cells implicated in learning and memory functions, they are also considered to be the major mediators of propofol activity. Accordingly, hippocampal neuron injury was observed in tissues. The results also demonstrated that $H_2S$ alleviated propofol-induced damage to hippocampal neurons, while the protective effect with 80 ppm $H_2S$ was more obvious than that with 40 ppm (Fig. 1E, $p < 0.01$). The aforementioned findings suggested that $H_2S$ could attenuate propofol-mediated toxicity in the hippocampal neurons. Furthermore, since the effect of 80 ppm $H_2S$ was more pronounced than that of 40 ppm $H_2S$, 80 ppm $H_2S$ was used for subsequent experiments to analyze the mechanism of regulation of $H_2S$.

### *$H_2S$ Promotes the Nuclear Translocation of Nrf2 and Alleviates Cell Apoptosis and Pyroptosis*

To further analyze the mechanism underlying the protective effect of $H_2S$ on propofol-induced hippocampal neuron injury, the rats were treated with different concen-

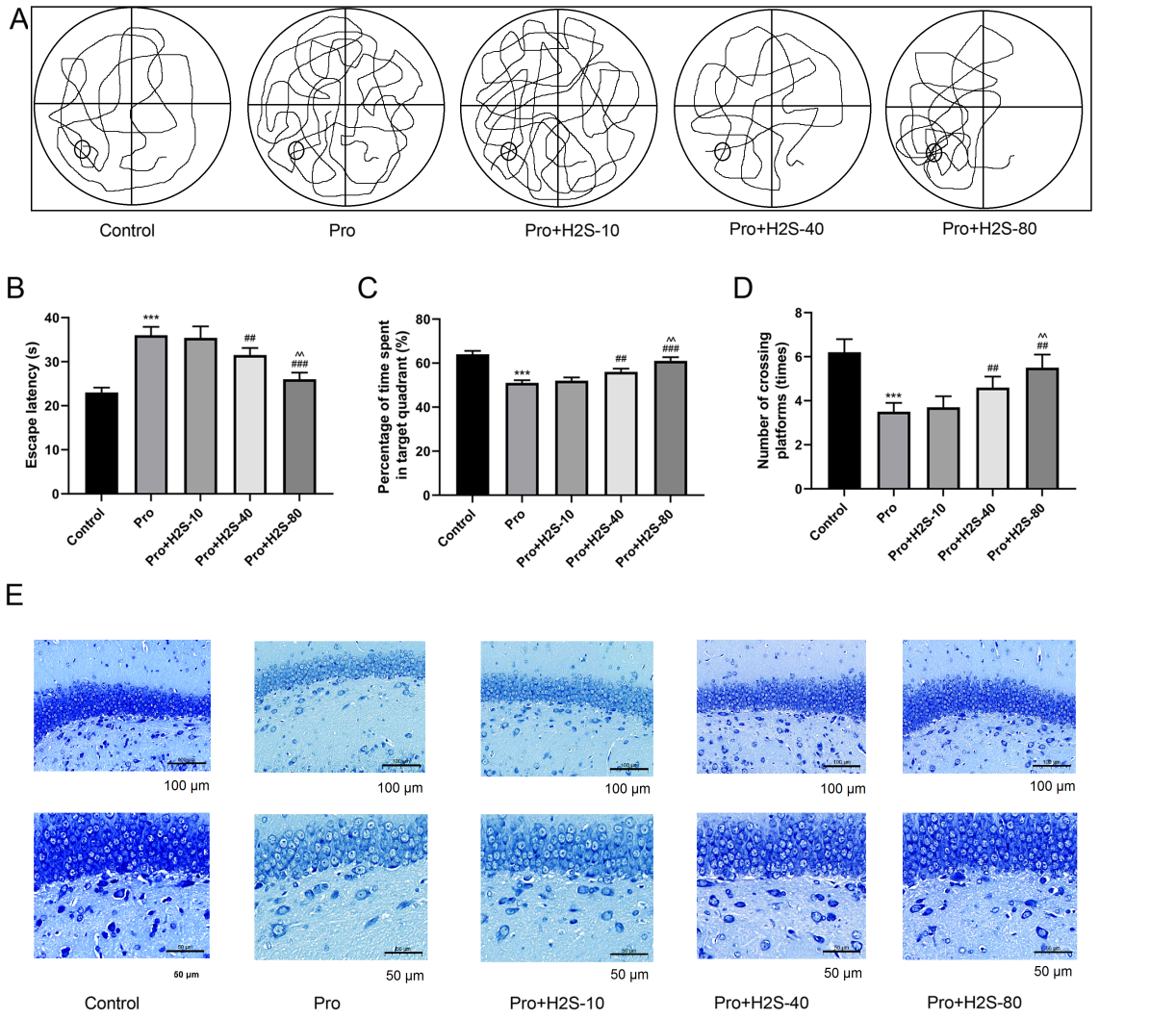


**Fig. 1. Hydrogen sulfide ($H_2S$) alleviates learning and memory dysfunction in propofol-treated rats.** (A–D) Morris water maze assay was performed to evaluate the effect of inhalation of 10, 40 and 80 ppm f $H_2S$ on learning and memory. (E) Nissl staining was used to evaluate the effects of different concentrations of $H_2S$ on hippocampal neuronal injury. $^{***}p < 0.001$ vs. the control group; $^{\#\#}p < 0.01$, and $^{\#\#\#}p < 0.001$ vs. the propofol (Pro) group; $^{\wedge\wedge}p < 0.01$ vs. Pro+$H_2S$-40 group. The data are expressed as the mean ± standard deviation (SD); N = 10.

trations of $H_2S$. Thereafter, cell apoptosis and pyroptosis were assessed. The results demonstrated that treatment with $H_2S$ inhibited the propofol-induced apoptosis in the rats in a dose-dependent manner ($p < 0.01$). However, the effect of 10 ppm $H_2S$ on cell apoptosis was not significant as compared to that of 80 ppm (Fig. 2A, $p > 0.05$). Propofol also upregulated NLRP3 and cleaved caspase-1 and GSDM-D in the hippocampal tissue ($p < 0.01$). However, exposure to 10 ppm $H_2S$ did not affect the expression of the above proteins. In contrast, both 40 and 80 ppm $H_2S$ inhibited propofol-induced NLRP3 activation and pyroptosis ($p < 0.01$). Interestingly, NLRP3-dependent pyroptosis significantly decreased in the Pro+$H_2S$-80 group as compared to that in the Pro+$H_2S$-40 group (Fig. 2B,C, $p < 0.01$). As described previously, the treatment of rats with propofol promotes the inhibition of *Nrf2*, which eventually results in cell apoptosis and pyroptosis. To this end, the nuclear translocation of the *Nrf2* protein was investigated further. The results demonstrated that propofol promoted *Nrf2* retention in the cytoplasm. However, treatment with 10 ppm $H_2S$ had no apparent effect on the localization of *Nrf2*. Furthermore, under propofol exposure, the inhalation of 40 and 80 ppm $H_2S$ significantly promoted the entry of *Nrf2* into the nucleus. Additionally, the nuclear (n)-*Nrf2*/cytoplasmatic (c)-*Nrf2* ratio was notably decreased in the Pro+$H_2S$-80 group as compared to that in the Pro+$H_2S$-40 group (Fig. 2D,E, $p < 0.01$). The aforementioned findings indicated that $H_2S$ could alleviate propofol-induced *Nrf2* inhibition and attenuate apoptosis and pyroptosis.

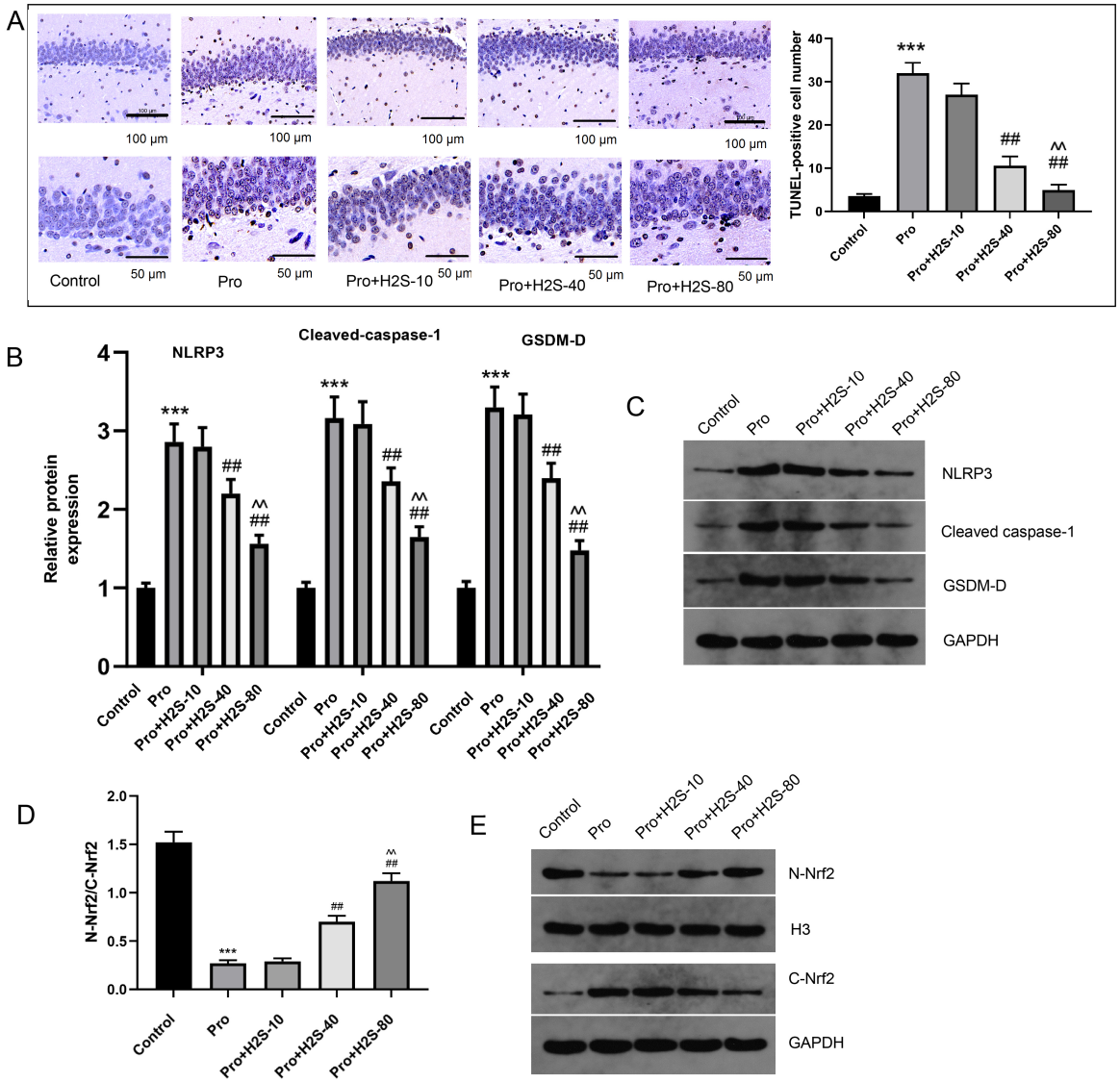


**Fig. 2. $H_2S$ promotes the nuclear translocation of nuclear factor erythroid 2-related factor 2 (*Nrf2*) and alleviates apoptosis and pyroptosis in hippocampal neurons.** (A) A TdT-mediated dUTP-biotin nick end labeling (TUNEL) assay was carried out to evaluate the effects of different $H_2S$ concentrations on the apoptosis of hippocampal neurons. (B,C) A comparison of the expression levels of NLR family pyrin domain containing 3 (NLRP3)-related pyroptosis markers in the hippocampus of rats is shown for each group. (D,E) Ratios of the nuclear *Nrf2* to Cytoplasmic *Nrf2* in the hippocampus of rats is shown for each group. $^{***}p < 0.001$ vs. the control group; $^{\#\#}p < 0.01$ vs. the Pro group; $^{\wedge\wedge}p < 0.01$ vs. the Pro+$H_2S$-40 group. H3, Histone H3; GSDM-D, gasdermin-D; GAPDH, Glyceraldehyde-3-phosphate dehydrogenase. The data are expressed as the mean ± SD; N = 10.

### *Nrf2 Silencing Abrogates the Protective Effects of $H_2S$ on Propofol-Induced Apoptosis*

To uncover the key role of *Nrf2* in mitigating propofol-related neurotoxicity via $H_2S$, *Nrf2*-deficient hippocampal neurons were established (Fig. 3A,B). To determine the optimal experimental concentration of propofol *in vitro*, hippocampal neurons were treated with 0, 100, 150 and 200 μmol/L of propofol. The results showed that treatment with ≤150 μmol/L propofol inhibited the viability of H19-7 cells in a dose-dependent manner ($p < 0.01$). Further, the inhibitory effects of 150 and 200 μmol/L propofol on cell viability were not significantly different (Fig. 3C, $p > 0.05$). Additionally, treatment with ≤150 μmol/L propofol inhibited the nuclear translocation of *Nrf2* in a dose-dependent manner (Fig. 3D,E, $p < 0.01$). Therefore, 150 μmol/L of propofol was used for the subsequent *in vitro* experiments. Furthermore, the cells were co-treated with 100, 200 and 400 μmol/L NaHS for 24 h to activate $H_2S$. All three $H_2S$ concentrations could promote the nuclear translocation of *Nrf2* ($p < 0.01$). Additionally, the n-*Nrf2*/c-*Nrf2* ratio was not significantly different between the groups that were treated with 200 and 400 μmol/L NaHS, $p > 0.05$). However, the n-*Nrf2*/c-*Nrf2* ratio was higher in the aforemen-

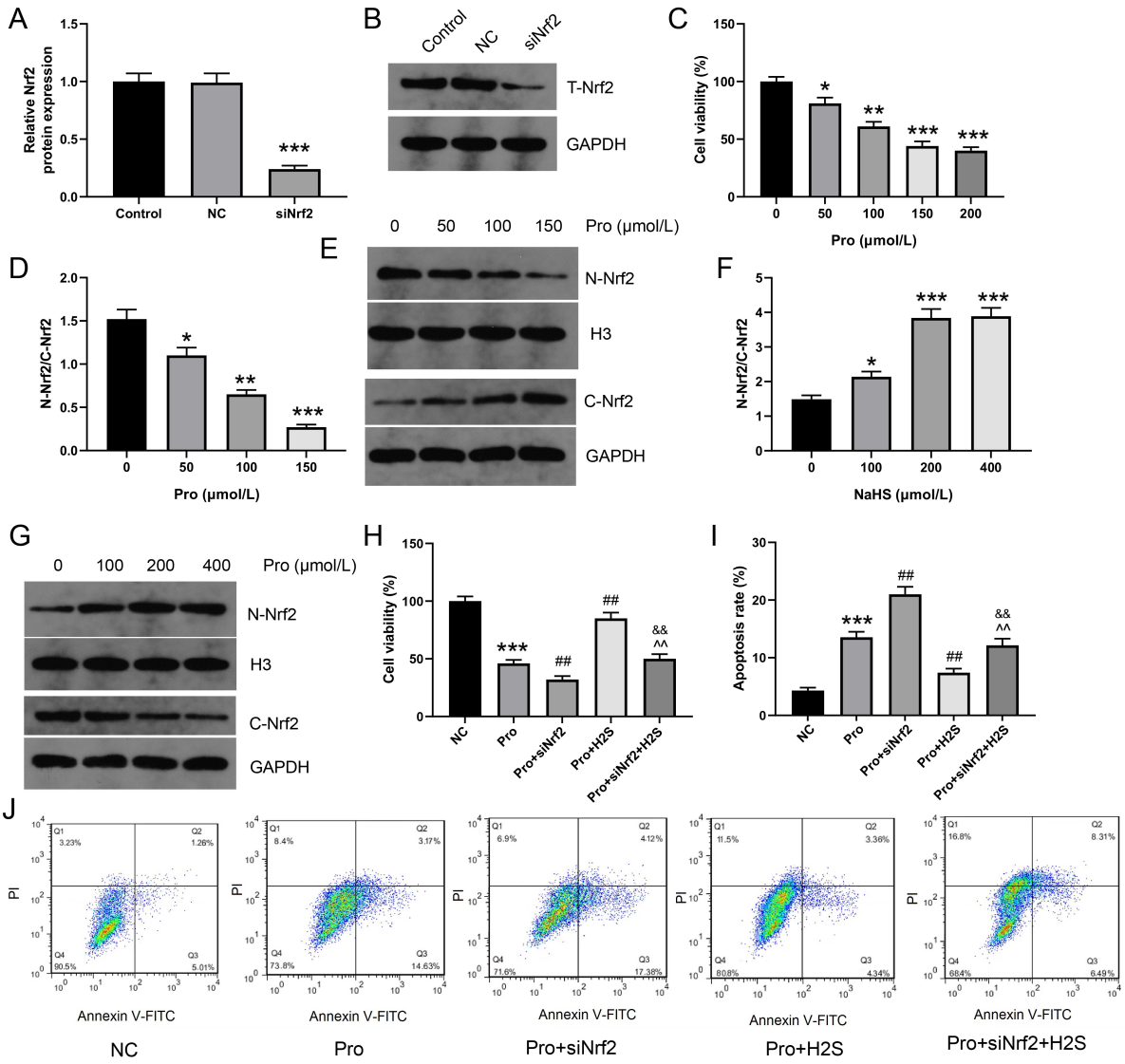


**Fig. 3. *Nrf2* silencing abrogates the protective effects of $H_2S$ on propofol-induced apoptosis in hippocampal neurons.** (A,B) Comparison of the transfection efficiency of H19-7 cells transfected with si-*Nrf2*. (C) The effects of different concentrations of propofol on the viability of H19-7 cells are shown here. (D,E) The effects of different concentrations of propofol on the nuclear translocation of *Nrf2* in H19-7 cells are shown here. (F,G) The effects of different concentrations of NaHS ($H_2S$ donor) on the nuclear translocation of *Nrf2* in H19-7 cells are presented here. (H) The effects of *Nrf2* silencing and exogenous $H_2S$ on the viability of cells treated with propofol are shown here. (I,J) The effects of *Nrf2* silencing and exogenous $H_2S$ on apoptosis of cells treated with propofol are shown here. $^{*}p < 0.05$ vs. the NC group; $^{**}p < 0.01$ vs. the negative control (NC) group; $^{***}p < 0.001$ vs. the NC group; $^{\#\#}p < 0.01$ vs. the Pro group; $^{\wedge\wedge}p < 0.01$ vs. the Pro+si*Nrf2* group; $^{\&\&}p < 0.01$ vs. the Pro+$H_2S$ group. Si-*Nrf2*, small interfering RNA against nuclear factor erythroid 2-related factor 2. The data are expressed as the mean ± SD; N = 3.

tioned groups compared with that in the 100 μmol/L group (Fig. 3F,G, $p < 0.01$). Finally, 200 μmol/L NaHS was used for subsequent experiments. Based on the above experiments, H19-7 cells were divided into the following five groups: NC, Pro (150 μmol/L) group, Pro+si*Nrf2*, Pro+$H_2S$ (200 μmol/L NaHS), and Pro+si*Nrf2*+$H_2S$ groups. *Nrf2* silencing further exacerbated the propofol-induced decrease in cell viability as well as apoptosis. In addition, $H_2S$ attenuated propofol-induced injury and apoptosis *in vitro* ($p < 0.01$). Furthermore, the protective effects of $H_2S$ on propofol-induced neurons were significantly inhibited following the knockdown of *Nrf2* (Fig. 3H–J, $p < 0.01$). The above results indicated that *Nrf2* silencing abrogated the protective effect of $H_2S$ on the hippocampal neurons, which supported the critical role of *Nrf2* in the mitigation of propofol-related neurotoxicity by $H_2S$.

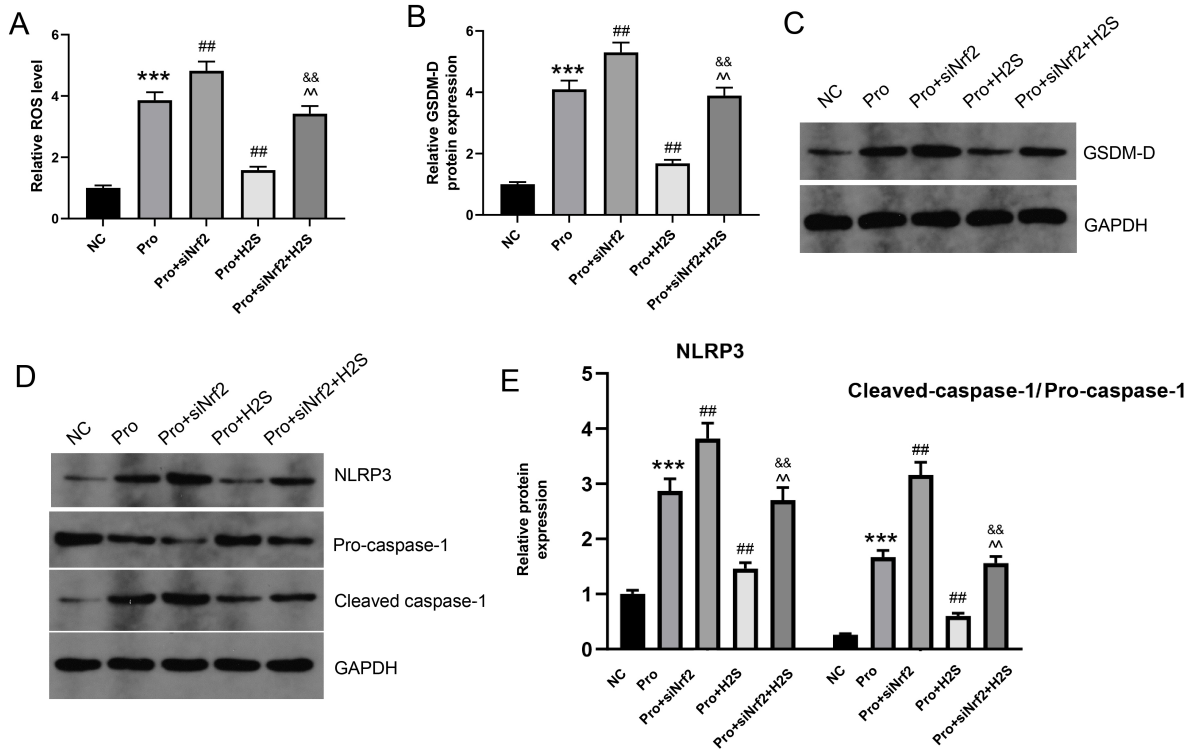


**Fig. 4. *Nrf2* silencing abrogates the protective effect of $H_2S$ on propofol-induced ROS production and NLRP3-dependent pyroptosis.** (A) The effects of *Nrf2* silencing and treatment with exogenous $H_2S$ on propofol-induced ROS production are shown here. (B,C) The effects of *Nrf2* knockdown and treatment with exogenous $H_2S$ on propofol-induced GSDM-D upregulation are shown here. (D,E) The effects of *Nrf2* silencing and treatment with exogenous $H_2S$ on propofol-induced activation of NLRP3 are shown here. $^{***}p < 0.001$ vs. the NC group; $^{\#\#}p < 0.01$ vs. the Pro group; $^{\wedge\wedge}p < 0.01$ vs. the Pro+si*Nrf2* group; $^{\&\&}p < 0.01$ vs. the Pro+$H_2S$. ROS, reactive oxygen species. The data are expressed as the mean ± SD; N = 3.

### *Nrf2 Knockdown Abrogates the Protective Effect of $H_2S$ against Propofol-Induced ROS Production and NLRP3-Dependent Pyroptosis*

The *in vitro* results in this study showed that H19-7 cell exposure to propofol led to the generation of ROS. Additionally, *Nrf2* silencing exacerbated propofol-induced oxidative stress, whereas $H_2S$ inhalation reduced the production of ROS. However, following cell transfection with si-*Nrf2*, the inhibitory effect of $H_2S$ on propofol-induced ROS production was alleviated (Fig. 4A, $p < 0.01$). Furthermore, $H_2S$ attenuated propofol-induced pyroptosis *in vitro*. Therefore, *Nrf2* knockdown aggravated propofol-induced pyroptosis as well as reversed the inhibitory effect of $H_2S$ on pyroptosis (Fig. 4B,C, $p < 0.01$). This finding indicated that *Nrf2* silencing could inhibit the protective effects of $H_2S$ on pyroptosis in hippocampal neurons. In addition, *Nrf2* silencing also exacerbated propofol-induced activation of the NLRP3 inflammasome and promoted the hydrolysis of pro-caspase-1 into active cleaved caspase-1 ($p < 0.01$). Overall, the results demonstrated that $H_2S$ inhibited NLRP3 activation, which was reversed by *Nrf2* silencing (Fig. 4D,E, $p < 0.01$). These findings suggested that the mechanism underlying the effect of $H_2S$ on the alleviation of propofol-induced pyroptosis was dependent on *Nrf2*.

### *Nrf2 Inhibition Reverses the Inhibitory Effect of $H_2S$ on the Activation of ROS and NLRP3 in Propofol-Induced Hippocampal Neurons in Rats*

To elucidate the critical role of *Nrf2* regarding the protective effects of $H_2S$ on propofol-induced oxidative stress and NLRP3 activation *in vivo*, rats were assigned into four groups as follows: control, Pro, Pro+$H_2S$ group, and Pro+$H_2S$+ML385 groups. The rats were treated with 80 ppm $H_2S$. The results demonstrated that the function of the *Nrf2* protein was inhibited by an intraperitoneal injection of ML385. Histological analysis of the hippocampal tissues revealed that ML385 inhibited $H_2S$-mediated *Nrf2* nuclear translocation *in vivo* (Fig. 5A,B, $p < 0.01$). Furthermore, $H_2S$ significantly inhibited the propofol-induced accumulation of ROS and NLRP3 activation. The inhibitory effect of $H_2S$ on ROS production and NLRP3 activation was significantly reduced when *Nrf2* function was inhibited by ML385 (Fig. 5C–E, $p < 0.01$). This finding verified that the mechanism underlying the effect of $H_2S$ on the alleviation of propofol-induced ROS production and NLRP3 activation was dependent on *Nrf2 in vivo*.

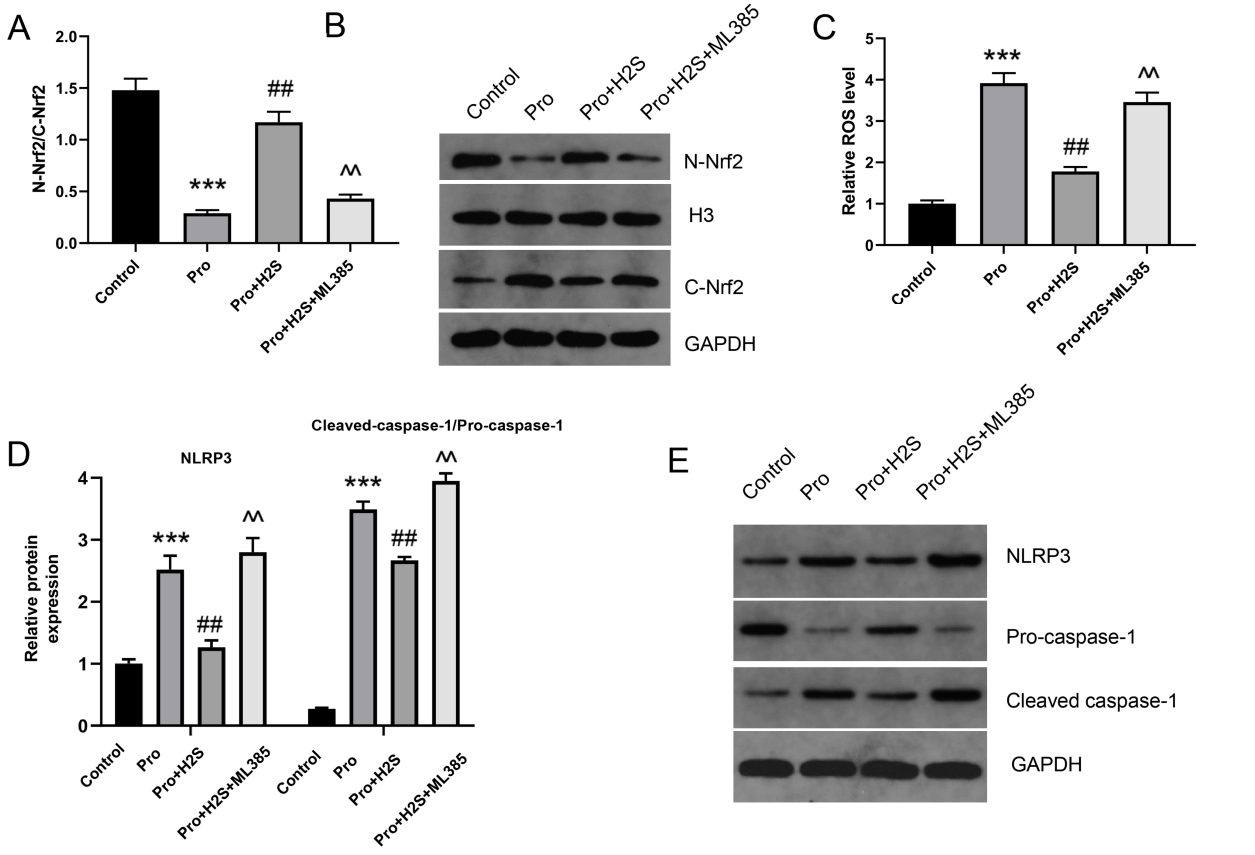


**Fig. 5. *Nrf2* inhibition attenuates the effect of $H_2S$ on propofol-induced activation of ROS and NLRP3 in rat hippocampal neurons.** (A,B) The effects of ML385 and $H_2S$ on propofol-induced nuclear translocation of *Nrf2* in rat hippocampal neurons are shown here. (C) The effects of *Nrf2* silencing and $H_2S$ on propofol-induced ROS production in hippocampal tissues are presented here. (D,E) The effects of *Nrf2* knockdown and $H_2S$ on propofol-induced activation of NLRP3 in hippocampal tissues are shown here. $^{***}p < 0.001$ vs. the control group; $^{\#\#}p < 0.01$ vs. the Pro group; $^{\wedge\wedge}p < 0.01$ vs. the Pro+$H_2S$ group. The data are expressed as the mean ± SD; N = 10.

### *Nrf2 Inhibition Blocks the Protective Effect of $H_2S$ on Propofol-Induced Hippocampal Neurons*

As previously described, exposure to 80 ppm $H_2S$ notably reduced propofol-induced nerve injury. Additionally, the protective effect of $H_2S$ on learning and memory dysfunction was attenuated with the inhibition of *Nrf2* (Fig. 6A–D, $p < 0.01$). The analysis of cell apoptosis revealed that $H_2S$ exposure decreased cell apoptosis in propofol-induced hippocampal neurons. However, the antiapoptotic effect of $H_2S$ was reversed with the inhibition of *Nrf2* (Fig. 7A,B, $p < 0.01$). In addition, GSDM-D was downregulated in the Pro+$H_2S$ group as compared to that in the Pro group. The protein expression levels of GSDM-D were significantly higher in the Pro+$H_2S$+ML385 group than that in the Pro+$H_2S$ group (Fig. 6C,D, $p < 0.01$). The aforementioned results suggested that *Nrf2* could play a central role in the mechanism underlying the effect of $H_2S$ on inhibiting propofol-induced hippocampal neuronal apoptosis and pyroptosis.

## Discussion

Propofol is commonly used in several conditions, which include painful examinations (gastroscopy), analgesia for tumors, and mechanical ventilation [29–31]. However, it has been reported that propofol adversely affects the development of the hippocampus [32,33]. Some studies have investigated possible solutions to prevent propofol-related neurotoxicity. For example, Shibuta *et al.* [34] examined the impact of preconditioning on the neurotoxicity caused by propofol during the developmental stage and discovered that propofol preconditioning did not reduce PPF-induced neural cell death under any circumstances. Moreover, another study demonstrated that Microrna-17-5p offered protection against neurotoxicity and impairment in autophagy caused by the use of propofol as anesthesia [35]. Additionally, lncRNA BDNF-AS was found to reduce propofol-induced apoptosis in HT22 cells by regulating the BDNF/TrkB pathway [36]. Xiao *et al.* [37] determined that dexmedetomidine mitigated the long-term neurotoxic effects of propofol on the developing brains of rats by amplifying the PI3K/Akt signaling pathway.

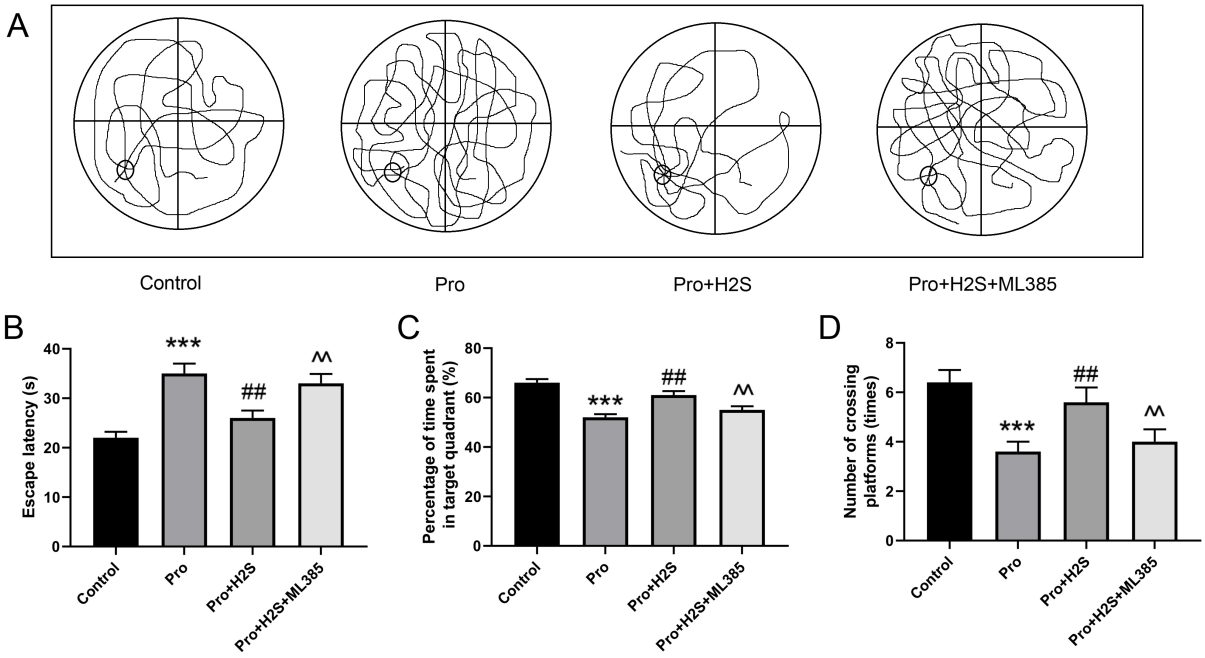


**Fig. 6. *Nrf2* inhibition abrogates the protective effect of $H_2S$ on propofol-induced impaired learning and memory.** Morris water maze assay was carried out to evaluate the effect of inhalation of 80 ppm $H_2S$ and *Nrf2* silencing on learning and memory. (A) Representative images of the Morris water maze assay are shown here. (B) Escape latency is demonstrated here. (C) The percentage of time spent in the target quadrant is presented here. (D) The number of times rats crossed platforms is shown here. $^{***}p < 0.001$ vs. the control group; $^{\#\#}p < 0.01$ vs. the Pro group; $^{\wedge\wedge}p < 0.01$ vs. the Pro+$H_2S$ group. The data are expressed as the mean ± SD; N = 10.

The body secretes specific levels of endogenous $H_2S$ generated by cysteine substances, and it acts via the dilation of blood vessels and regulation of energy metabolism [38,39]. $H_2S$ is also involved in nerve conduction for the protection of nerve function. Further, it enhances calcium influx by regulating the N-methyl-D-aspartate receptors [40], which serve a significant role in hippocampal long-term potentiation and memory [41]. Another study demonstrated that $H_2S$ could alleviate Alzheimer's disease by regulating glycogen synthase kinase 3$\beta$ [42]. Furthermore, $H_2S$ could also attenuate anxiety and depression in animals by upregulating Sirtuin 1 in the hippocampus [43]. To investigate whether $H_2S$ could alleviate propofol-induced toxicity in hippocampal neurons, rats were treated with inhalation of 10, 40 and 80 ppm $H_2S$. The water maze assay revealed that exposure to propofol for up to 8 weeks could affect the ability of rats to find the underwater platforms. Additionally, Nissl staining results showed that propofol induced neuronal injury. Although the inhalation of 10 ppm $H_2S$ could not alleviate the above effects, treatment with 40 and 80 ppm $H_2S$ notably attenuated propofol-induced injury in the hippocampal neurons. The protective effect of 80 ppm $H_2S$ was more evident as compared to that of 40 ppm. This may also be due to the fatigue-like effects of high concentrations of $H_2S$ in rats. The safety and toxicity of $H_2S$ in rats require to be analyzed further. These findings suggested that $H_2S$ could alleviate propofol-related neurotoxicity *in vivo*.

Subsequently, the current study aimed to elucidate the mechanism of propofol-induced hippocampal injury as well as the ameliorating effect of $H_2S$. The results verified that propofol could induce the accumulation of ROS by inhibiting *Nrf2* function, thereby promoting neuronal cell apoptosis [44,45]. It has been reported that ROS is a key factor in the activation of NLRP3-related pyroptosis [46,47]. Further, apoptosis and pyroptosis of the hippocampal neurons can directly impair neuronal function, thereby affecting learning and memory abilities. Hence, inhibiting apoptosis and pyroptosis is considered a key step in improving learning and memory [48,49]. The results of the current study demonstrated that inhalation of 40 and 80 ppm $H_2S$ inhibited propofol-induced apoptosis as well as cell pyroptosis. The inhibitory effects of 80 ppm $H_2S$ were more potent as compared to those of 40 ppm. Furthermore, $H_2S$ inhalation also promotes the nuclear translocation of *Nrf2*. After entry into the nucleus, *Nrf2* promotes the transcription of the superoxide dismutase (SOD) antioxidant factor and eventually inhibits the accumulation of ROS, which in turn attenuates cell apoptosis and pyroptosis [50,51]. Patra *et al.* [22] found that a decline in *Nrf2* coincided with the active nuclear absence of *Nrf2*, leading to decreased expression of *Nrf2* target genes like heme oxygenase-1 (HO-1), NAD(P)H quinone dehydrogenase 1, and SOD1. Additionally, Ying *et al.* [23] studied *Nrf2* knockdown in cells and demonstrated that for the initiation of an effective innate defense response, *Nrf2* was crucial for primary bovine mam-

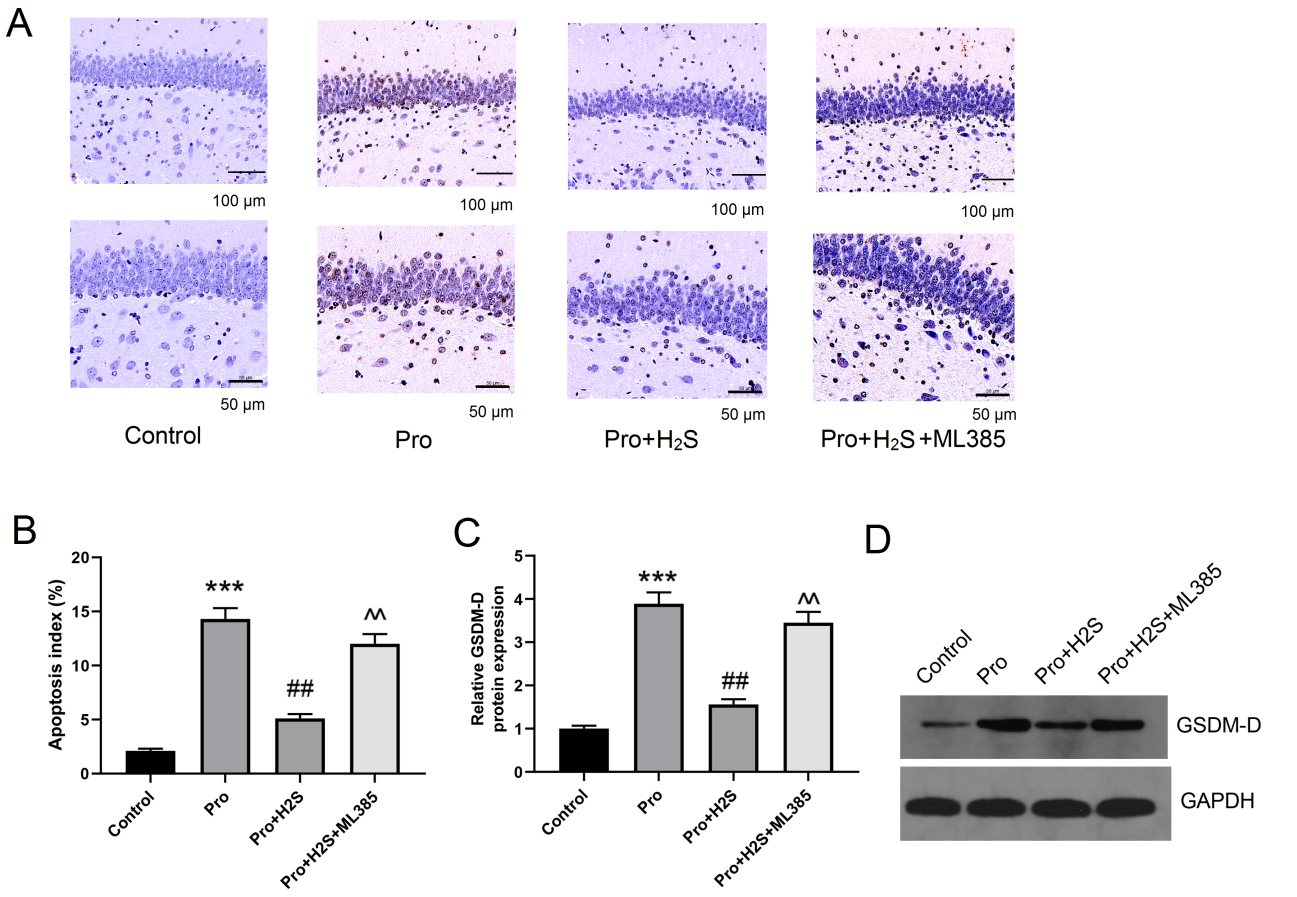


**Fig. 7. *Nrf2* knockdown attenuates the effect of $H_2S$ on propofol-induced apoptosis and pyroptosis in hippocampal neurons.** TUNEL assay was used to detect the apoptosis rate of hippocampal neurons. To assess the effects of inhalation of 80 ppm $H_2S$ and *Nrf2* silencing on pyroptosis in hippocampal neurons, the expression levels of gasdermin-D were determined using Western blot analysis. (A) Representative images of the TUNEL assay are shown here. (B) TUNEL assay results are shown here. (C) The relative protein expression levels of GSMD-D are presented here. (D) Representative Western blot analysis results are shown. $^{***}p < 0.001$ vs. the control group; $^{\#\#}p < 0.01$ vs. the Pro group; $^{\wedge\wedge}p < 0.01$ vs. the Pro+$H_2S$ group. The data are expressed as the mean ± SD; N = 10.

mary epithelial cells. Further, the overexpression of nuclear *Nrf2* intensified the inflammatory response triggered by S. aureus, which is an unusual factor causing various infections [23]. This may also be an underlying mechanism for brain injury protection. $H_2S$ is involved in regulating *Nrf2* and ameliorating fatty liver injury, ischemic myocardial injury, and traumatic brain injury via the activation of *Nrf2* [52,53]. The aforementioned findings preliminarily suggested that $H_2S$ could alleviate propofol-induced learning and memory impairment by activating *Nrf2* to inhibit cell apoptosis and pyroptosis.

To elucidate the mechanism by which *Nrf2* alleviates propofol-induced neurotoxicity via $H_2S$, *in vitro* rescue experiments were carried out using *Nrf2*-deficient H19-7 cells. $H_2S$ was produced using a culture medium supplemented with NaHS. The rescue experiments revealed that the inhibition of *Nrf2* expression not only aggravated propofol-induced cell pyroptosis and apoptosis but also abrogated the protective effects of $H_2S$. Finally, *in vivo* experiments also demonstrated that inhibition of *Nrf2* reversed the protective effects of $H_2S$ inhalation on learning and memory as well as propofol-induced cell apoptosis. These findings suggested that the mechanism underlying the effect of $H_2S$ on the alleviation of pyroptosis and apoptosis and protection of hippocampal function were inseparable from *Nrf2*. Some other studies have also reported the effect of $H_2S$ in apoptosis and pyroptosis. Hu *et al.* [54] found that $H_2S$ attenuated uranium-induced pyroptosis in kidney cells. Further, Zhang *et al.* [55] discovered that an injectable silk fibroin (SF)-based hydrogel with continuous $H_2S$ delivery reduced neuronal pyroptosis and improved functional recovery after severe intracerebral hemorrhage. In another study, it was demonstrated that $H_2S$ mitigated pyroptosis induced by cigarette smoke via the TLR4/NF-$\kappa$B signaling pathway [15]. Cheng *et al.* [56] showed that NaHS, which is an external $H_2S$ donor, significantly enhanced cell viability, reduced apoptosis ratio, and decreased caspase-3 activity along with the Bax/Bcl-2 ratio in PC12 cells that

were exposed to arecoline. All these studies suggested the regulation of apoptosis and pyroptosis via $H_2S$.

The present study had some limitations. First, regarding propofol, the *in vivo* environment and *in vitro* cellular environment of clinical patients are different. Second, only one cell type was used in the current study to verify the effects of propofol and NaHS. In addition, no pyroptosis/NLRP3 inhibitors were used for the rescue experiments. Our next research focus would be to investigate the effect of $H_2S$ on regulating *Nrf2*. However, the current study only analyzed the mechanism based on the *Nrf2* pathway, and other mechanisms of $H_2S$ require to be studied further. In addition, inhibiting cell apoptosis and pyroptosis may not be the only mechanism for the effects of $H_2S$. Hence, other mechanisms involved should also be explored in future studies. Regarding the clinical application of $H_2S$, it may be administered as NaHS, through $H_2S$ inhalation, or via an $H_2S$ donor. However, their concentration and safety for clinical application need to be studied.

## Conclusions

In conclusion, the current study suggested that repeated exposure to propofol could promote hippocampal neuronal apoptosis and pyroptosis by inhibiting the nuclear translocation of *Nrf2*. Additionally, $H_2S$ could protect neural function by activating *Nrf2*. Further, administering $H_2S$ could be used as a novel approach in clinical settings for protecting the learning and memory abilities of patients treated with propofol. Therefore, propofol-treated patients could be administered with $H_2S$ inhalation to protect their learning and memory abilities. However, the route of administration of $H_2S$, its pharmacodynamic relationship and toxicity, and the mechanism underlying the effect of $H_2S$ on the alleviation of propofol-induced neurotoxicity should be investigated further. The possible applications of $H_2S$ in clinical settings include gas inhalation, NaHS delivery, or silk fibroin-based hydrogel with sustained $H_2S$ delivery.

## Availability of Data and Materials

The datasets used and/or analyzed for this study are available from the corresponding author upon reasonable request.

## Author Contributions

ZL, YW, XW, MF and BG designed the research study. ZL performed the animal experiments and drafted the manuscript. YW and XW performed the *in vitro* experiments. MF analyzed the data. BG contributed to the supervision of the study and revised the manuscript. All authors contributed to editorial changes in the manuscript. All authors read and approved the final manuscript. All authors have participated sufficiently in the work and agreed to be accountable for all aspects of the work.

## Ethics Approval and Consent to Participate

All experimental protocols were approved by the Animal Care Committee of Shandong Provincial Third Hospital (No. DWKYLL-2020008).

## Acknowledgment

Not applicable.

## Funding

This research received no external funding.

## Conflict of Interest

The authors declare no conflict of interest.

## References

[1] Li Y, Chen D, Wang H, Wang Z, Song F, Li H, *et al*. Intravenous versus Volatile Anesthetic Effects on Postoperative Cognition in Elderly Patients Undergoing Laparoscopic Abdominal Surgery. Anesthesiology. 2021; 134: 381–394.

[2] Pang QY, Duan LP, Jiang Y, Liu HL. Effects of inhalation and propofol anaesthesia on postoperative cognitive dysfunction in elderly noncardiac surgical patients: A systematic review and meta-analysis. Medicine. 2021; 100: e27668.

[3] Stogiannou D, Protopapas A, Protopapas A, Tziomalos K. Is propofol the optimal sedative in gastrointestinal endoscopy? Acta Gastro-enterologica Belgica. 2018; 81: 520–524.

[4] Li XT, Ma CQ, Qi SH, Zhang LM. Combination of propofol and dezocine to improve safety and efficacy of anesthesia for gastroscopy and colonoscopy in adults: A randomized, double-blind, controlled trial. World Journal of Clinical Cases. 2019; 7: 3237–3246.

[5] Wan J, Shen CM, Wang Y, Wu QZ, Wang YL, Liu Q, *et al*. Repeated exposure to propofol in the neonatal period impairs hippocampal synaptic plasticity and the recognition function of rats in adulthood. Brain Research Bulletin. 2021; 169: 63–72.

[6] Wang Y, Wu C, Han B, Xu F, Mao M, Guo X, *et al*. Dexmedetomidine attenuates repeated propofol exposure-induced hippocampal apoptosis, PI3K/Akt/Gsk-3$\beta$ signaling disruption, and juvenile cognitive deficits in neonatal rats. Molecular Medicine Reports. 2016; 14: 769–775.

[7] Liu PF, Gao T, Li TZ, Yang YT, Xu YX, Xu ZP, *et al*. Repeated propofol exposure-induced neuronal damage and cognitive impairment in aged rats by activation of NF-κB pathway and NLRP3 inflammasome. Neuroscience Letters. 2021; 740: 135461.

[8] Tang F, Zhao L, Yu Q, Liu T, Gong H, Liu Z, *et al*. Upregulation of miR-215 attenuates propofol-induced apoptosis and oxidative stress in developing neurons by targeting LATS2. Molecular Medicine. 2020; 26: 38.

[9] Zhang Z, Xu Y, Chi S, Cui L. MicroRNA-582-5p Reduces Propofol-induced Apoptosis in Developing Neurons by Targeting ROCK1. Current Neurovascular Research. 2020; 17: 140–146.

[10] Liang C, Du F, Cang J, Xue Z. Pink1 attenuates propofol-induced apoptosis and oxidative stress in developing neurons. Journal of Anesthesia. 2018; 32: 62–69.

[11] Minutoli L, Puzzolo D, Rinaldi M, Irrera N, Marini H, Arcoraci V, *et al*. ROS-Mediated NLRP3 Inflammasome Activation

in Brain, Heart, Kidney, and Testis Ischemia/Reperfusion Injury. Oxidative Medicine and Cellular Longevity. 2016; 2016: 2183026.

[12] Teng JF, Mei QB, Zhou XG, Tang Y, Xiong R, Qiu WQ, *et al*. Polyphyllin VI Induces Caspase-1-Mediated Pyroptosis via the Induction of ROS/NF-κB/NLRP3/GSDMD Signal Axis in Non-Small Cell Lung Cancer. Cancers. 2020; 12: 193.

[13] Jiang S, Gu H, Zhao Y, Sun L. Teleost Gasdermin E Is Cleaved by Caspase 1, 3, and 7 and Induces Pyroptosis. Journal of Immunology. 2019; 203: 1369–1382.

[14] Sun L, Ma W, Gao W, Xing Y, Chen L, Xia Z, *et al*. Propofol directly induces caspase-1-dependent macrophage pyroptosis through the NLRP3-ASC inflammasome. Cell Death & Disease. 2019; 10: 542.

[15] Wang L, Meng J, Wang C, Wang Y, Yang C, Li Y. Hydrogen sulfide attenuates cigarette smoke induced pyroptosis through the TLR4/NF κB signaling pathway. International Journal of Molecular Medicine. 2022; 49: 56.

[16] Ni J, Jiang L, Shen G, Xia Z, Zhang L, Xu J, *et al*. Hydrogen sulfide reduces pyroptosis and alleviates ischemia-reperfusion-induced acute kidney injury by inhibiting NLRP3 inflammasome. Life Sciences. 2021; 284: 119466.

[17] Mata A, Cadenas S. The Antioxidant Transcription Factor Nrf2 in Cardiac Ischemia-Reperfusion Injury. International Journal of Molecular Sciences. 2021; 22: 11939.

[18] Friedmann Angeli JP, Meierjohann S. NRF2-dependent stress defense in tumor antioxidant control and immune evasion. Pigment Cell & Melanoma Research. 2021; 34: 268–279.

[19] Bian H, Wang G, Huang J, Liang L, Zheng Y, Wei Y, *et al*. Dihydrolipoic acid protects against lipopolysaccharide-induced behavioral deficits and neuroinflammation via regulation of Nrf2/HO-1/NLRP3 signaling in rat. Journal of Neuroinflammation. 2020; 17: 166.

[20] Harvey CJ, Thimmulappa RK, Sethi S, Kong X, Yarmus L, Brown RH, *et al*. Targeting Nrf2 signaling improves bacterial clearance by alveolar macrophages in patients with COPD and in a mouse model. Science Translational Medicine. 2011; 3: 78ra32.

[21] Song CH, Kim N, Nam RH, Choi SI, Yu JE, Nho H, *et al*. Changes in Microbial Community Composition Related to Sex and Colon Cancer by Nrf2 Knockout. Frontiers in Cellular and Infection Microbiology. 2021; 11: 636808.

[22] Patra U, Mukhopadhyay U, Mukherjee A, Sarkar R, Chawla-Sarkar M. Progressive Rotavirus Infection Downregulates Redox-Sensitive Transcription Factor Nrf2 and Nrf2-Driven Transcription Units. Oxidative Medicine and Cellular Longevity. 2020; 2020: 7289120.

[23] Ying YT, Yang J, Tan X, Liu R, Zhuang Y, Xu JX, *et al*. *Escherichia coli* and *Staphylococcus aureus* Differentially Regulate Nrf2 Pathway in Bovine Mammary Epithelial Cells: Relation to Distinct Innate Immune Response. Cells. 2021; 10: 3426.

[24] Xie L, Gu Y, Wen M, Zhao S, Wang W, Ma Y, *et al*. Hydrogen Sulfide Induces Keap1 S-sulfhydration and Suppresses Diabetes-Accelerated Atherosclerosis via Nrf2 Activation. Diabetes. 2016; 65: 3171–3184.

[25] Li Y, Chandra TP, Song X, Nie L, Liu M, Yi J, *et al*. H2S improves doxorubicin-induced myocardial fibrosis by inhibiting oxidative stress and apoptosis via Keap1-Nrf2. Technology and Health Care. 2021; 29: 195–209.

[26] Ji K, Xue L, Cheng J, Bai Y. Preconditioning of H2S inhalation protects against cerebral ischemia/reperfusion injury by induction of HSP70 through PI3K/Akt/Nrf2 pathway. Brain Research Bulletin. 2016; 121: 68–74.

[27] Feng LX, Zhao F, Liu Q, Peng JC, Duan XJ, Yan P, *et al*. Role of Nrf2 in Lipopolysaccharide-Induced Acute Kidney Injury: Protection by Human Umbilical Cord Blood Mononuclear Cells. Oxidative Medicine and Cellular Longevity. 2020; 2020: 6123459.

[28] Yang Y, Yi J, Pan M, Hu B, Duan H. Edaravone Alleviated Propofol-Induced Neurotoxicity in Developing Hippocampus by mBDNF/TrkB/PI3K Pathway. Drug Design, Development and Therapy. 2021; 15: 1409–1422.

[29] Strøm T, Martinussen T, Toft P. A protocol of no sedation for critically ill patients receiving mechanical ventilation: a randomised trial. Lancet. 2010; 375: 475–480.

[30] Zou J, Zhang Z, Mao Q. Application of butorphanol tartrate combined with propofol in painless gastroscopy. Minerva Medica. 2021. (online ahead of print)

[31] Guerrero Orriach JL, Raigon Ponferrada A, Malo Manso A, Herrera Imbroda B, Escalona Belmonte JJ, Ramirez Aliaga M, *et al*. Anesthesia in Combination with Propofol Increases Disease-Free Survival in Bladder Cancer Patients Who Undergo Radical Tumor Cystectomy as Compared to Inhalational Anesthetics and Opiate-Based Analgesia. Oncology. 2020; 98: 161–167.

[32] Jacob Z, Li H, Makaryus R, Zhang S, Reinsel R, Lee H, *et al*. Metabolomic profiling of children's brains undergoing general anesthesia with sevoflurane and propofol. Anesthesiology. 2012; 117: 1062–1071.

[33] Zhu X, Li H, Tian M, Zhou S, He Y, Zhou M. miR-455-3p alleviates propofol-induced neurotoxicity by reducing EphA4 expression in developing neurons. Biomarkers. 2020; 25: 685–692.

[34] Shibuta S, Morita T, Kosaka J. Effect of preconditioning on propofol-induced neurotoxicity during the developmental period. PLoS ONE. 2022; 17: e0273219.

[35] Xiu M, Luan H, Gu X, Liu C, Xu D. MicroRNA-17-5p Protects against Propofol Anesthesia-Induced Neurotoxicity and Autophagy Impairment via Targeting BCL2L11. Computational and Mathematical Methods in Medicine. 2022; 2022: 6018037.

[36] Xu YH, Luo Y, Cao JB, Liu YH, Song YX, Zhang XY, *et al*. lncRNA BDNF-AS Attenuates Propofol-Induced Apoptosis in HT22 Cells by Modulating the BDNF/TrkB Pathway. Molecular Neurobiology. 2022; 59: 3504–3511.

[37] Xiao Y, Zhou L, Tu Y, Li Y, Liang Y, Zhang X, *et al*. Dexmedetomidine attenuates the propofol-induced long-term neurotoxicity in the developing brain of rats by enhancing the PI3K/Akt signaling pathway. Neuropsychiatric Disease and Treatment. 2018; 14: 2191–2206.

[38] Szabo C. Hydrogen Sulfide, an Endogenous Stimulator of Mitochondrial Function in Cancer Cells. Cells. 2021; 10: 220.

[39] Li P, Liu H, Shi X, Prokosch V. Hydrogen Sulfide: Novel Endogenous and Exogenous Modulator of Oxidative Stress in Retinal Degeneration Diseases. Molecules. 2021; 26: 2411.

[40] Sone K, Mori A, Sakamoto K, Nakahara T. GYY4137, an Extended-Release Hydrogen Sulfide Donor, Reduces NMDA-Induced Neuronal Injury in the Murine Retina. Biological & Pharmaceutical Bulletin. 2018; 41: 657–660.

[41] Kang J, Kadam SD, Elmore JS, Sullivan BJ, Valentine H, Malla AP, *et al*. Transcranial photoacoustic imaging of NMDA-evoked focal circuit dynamics in the rat hippocampus. Journal of Neural Engineering. 2020; 17: 025001.

[42] Giovinazzo D, Bursac B, Sbodio JI, Nalluru S, Vignane T, Snowman AM, *et al*. Hydrogen sulfide is neuroprotective in Alzheimer's disease by sulfhydrating GSK3$\beta$ and inhibiting Tau hyperphosphorylation. Proceedings of the National Academy of Sciences of the United States of America. 2021; 118: e2017225118.

[43] Kang X, Jiang L, Lan F, Tang YY, Zhang P, Zou W, *et al*. Hydrogen sulfide antagonizes sleep deprivation-induced depression- and anxiety-like behaviors by inhibiting neuroinflammation in a hippocampal Sirt1-dependent manner. Brain Research Bulletin. 2021; 177: 194–202.

[44] Zhang Z, Yan B, Li Y, Yang S, Li J. Propofol inhibits oxidative stress injury through the glycogen synthase kinase 3 beta/nuclear factor erythroid 2-related factor 2/heme oxygenase-1 signaling pathway. Bioengineered. 2022; 13: 1612–1625.

[45] Zhang L, Zhou Q, Zhou CL. RTA-408 protects against propofol-induced cognitive impairment in neonatal mice via the activation of Nrf2 and the inhibition of NF-κB p65 nuclear translocation. Brain and Behavior. 2021; 11: e01918.

[46] Tang YS, Zhao YH, Zhong Y, Li XZ, Pu JX, Luo YC, *et al*. Neferine inhibits LPS-ATP-induced endothelial cell pyroptosis via regulation of ROS/NLRP3/Caspase-1 signaling pathway. Inflammation Research. 2019; 68: 727–738.

[47] Cheng YC, Chu LW, Chen JY, Hsieh SL, Chang YC, Dai ZK, *et al*. Loganin Attenuates High Glucose-Induced Schwann Cells Pyroptosis by Inhibiting ROS Generation and NLRP3 Inflammasome Activation. Cells. 2020; 9: 1948.

[48] Tang JJ, Feng S, Chen XD, Huang H, Mao M, Wang HY, *et al*. The Effects of P75NTR on Learning Memory Mediated by Hippocampal Apoptosis and Synaptic Plasticity. Current Pharmaceutical Design. 2021; 27: 531–539.

[49] Song X, Cui Z, He J, Yang T, Sun X. κ opioid receptor agonist, U50488H, inhibits pyroptosis through NLRP3 via the $Ca^{2+}$/CaMKII/CREB signaling pathway and improves synaptic plasticity in APP/PS1 mice. Molecular Medicine Reports. 2021; 24: 529.

[50] Liu M, Zhang C, Xu X, Zhao X, Han Z, Liu D, *et al*. Ferulic acid inhibits LPS-induced apoptosis in bovine mammary epithelial cells by regulating the NF-κB and Nrf2 signalling pathways to restore mitochondrial dynamics and ROS generation. Veterinary Research. 2021; 52: 104.

[51] Diao C, Chen Z, Qiu T, Liu H, Yang Y, Liu X, *et al*. Inhibition of PRMT5 Attenuates Oxidative Stress-Induced Pyroptosis via Activation of the Nrf2/HO-1 Signal Pathway in a Mouse Model of Renal Ischemia-Reperfusion Injury. Oxidative Medicine and Cellular Longevity. 2019; 2019: 2345658.

[52] Zhang J, Shi C, Wang H, Gao C, Chang P, Chen X, *et al*. Hydrogen sulfide protects against cell damage through modulation of PI3K/Akt/Nrf2 signaling. The International Journal of Biochemistry & Cell Biology. 2019; 117: 105636.

[53] Wang H, Shi X, Cheng L, Han J, Mu J. Hydrogen sulfide restores cardioprotective effects of remote ischemic preconditioning in aged rats *via* HIF-1$\alpha$/Nrf2 signaling pathway. The Korean Journal of Physiology & Pharmacology. 2021; 25: 239–249.

[54] Hu Q, Zhang R, Zheng J, Song M, Gu C, Li W. Hydrogen sulfide attenuates uranium-induced kidney cells pyroptosis via upregulation of PI3K/AKT/mTOR signaling. Journal of Biochemical and Molecular Toxicology. 2023; 37: e23220.

[55] Zhang J, Li S, Yang Z, Liu C, Chen X, Zhang Y, *et al*. Implantation of injectable SF hydrogel with sustained hydrogen sulfide delivery reduces neuronal pyroptosis and enhances functional recovery after severe intracerebral hemorrhage. Biomaterials Advances. 2022; 135: 212743.

[56] Cheng X, Jiang JM, Wang CY, Zou W, Zhang P, Tang XQ. Hydrogen sulfide prevents arecoline-induced neurotoxicity via promoting leptin/leptin receptor signaling pathway. Cell Biology International. 2022; 46: 1355–1366.